

# Journal of Materials Chemistry A

Accepted Manuscript



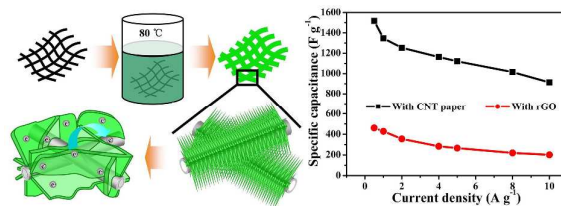
This is an *Accepted Manuscript*, which has been through the Royal Society of Chemistry peer review process and has been accepted for publication.

*Accepted Manuscripts* are published online shortly after acceptance, before technical editing, formatting and proof reading. Using this free service, authors can make their results available to the community, in citable form, before we publish the edited article. We will replace this *Accepted Manuscript* with the edited and formatted *Advance Article* as soon as it is available.

You can find more information about *Accepted Manuscripts* in the [Information for Authors](#).

Please note that technical editing may introduce minor changes to the text and/or graphics, which may alter content. The journal's standard [Terms & Conditions](#) and the [Ethical guidelines](#) still apply. In no event shall the Royal Society of Chemistry be held responsible for any errors or omissions in this *Accepted Manuscript* or any consequences arising from the use of any information it contains.

## Table of Contents



Amorphous Ni<sub>2</sub>(OH)<sub>2</sub>CO<sub>3</sub> nanowire arrays on a CNT paper were electrochemically converted into Ni(OH)<sub>2</sub> nanosheet with high capacitance for supercapacitors.

Cite this: DOI: 10.1039/c0xx00000x

www.rsc.org/xxxxxx

ARTICLE TYPE

# Electrochemical conversion of $\text{Ni}_2(\text{OH})_2\text{CO}_3$ into $\text{Ni}(\text{OH})_2$ hierarchical nanostructures loaded on carbon nanotube paper with highly electrochemical energy storage performance

Hongyuan Chen,<sup>a,b</sup> Yiran Kang,<sup>a,b,c</sup> Feng Cai,<sup>a,b,d</sup> Sha Zeng,<sup>a,b,e</sup> Weiwei Li,<sup>a,b</sup> Minghai Chen,<sup>a,b\*</sup> and Qingwen Li<sup>a,b\*</sup>

Received (in XXX, XXX) Xth XXXXXXXXX 20XX, Accepted Xth XXXXXXXXX 20XX

DOI: 10.1039/b000000x

**Large-diameter carbon nanotube (CNT) paper was used as a porous and conductive template to form vertically aligned  $\text{Ni}_2(\text{OH})_2\text{CO}_3$  nanowire array shells, which could be further converted into highly active  $\text{Ni}(\text{OH})_2$  nanosheets by cyclic voltammetry strategy. The as-prepared hierarchical nanostructure showed superior electrochemical performance for the electrodes of supercapacitors.**

Recently, electrochemical supercapacitors have attracted much attention among electrochemical energy storage devices, for its high power density and long life time.<sup>1</sup> However, most of commercialized supercapacitors were porous carbon symmetric supercapacitors based on electrochemical double-layer energy storage mechanism, which could largely limit the specific capacitance of the devices.<sup>2</sup> Pseudocapacitive materials with large capacitances and energies could be an excellent coordination of carbonaceous materials for highly capacitive supercapacitors.<sup>3</sup> Among various pseudocapacitive materials, nickel base hydroxides have ultra-high specific capacitance comparing with active carbon, thus were usually investigated as pseudocapacitive materials for the electrodes of asymmetric supercapacitors.<sup>4</sup> However, their low conductivity largely decreased their practical capacitance and rate performance. Their growth on conductive scaffolds such as nickel foam,<sup>5</sup> carbon fiber paper<sup>6</sup> and carbon nanotube (CNT) paper<sup>7</sup> may resolve this problem in a certain extend, but the pristine grown  $\text{Ni}(\text{OH})_2$  nanosheets were thick with small specific area, which may reduce their contact area with electrolyte.<sup>8</sup> As a result, the practical capacitance was still low. In this research, ultra-thin amorphous  $\text{Ni}_2(\text{OH})_2\text{CO}_3$  nanowire arrays were grown on individual CNTs in a CNT paper with large mass loading. These nanowires were in-situ converted into  $\text{Ni}(\text{OH})_2$  nanosheets by electrochemical cyclic reaction. The hybrid paper shows high specific capacitance, thus may serve as a promising candidate for the electrodes of high-performance asymmetric supercapacitors.

Multi-walled CNTs (MWCNTs) with large diameters (50–150 nm) were assembled to a porous paper by dispersion in aqueous solution and then vacuum filtration process.<sup>9</sup> This CNT paper was immersed into an aqueous solution with  $\text{NiCl}_2$  and urea and then heated to 80 °C for 24 h (as shown in Figure

1a. After that, the as-prepared paper with large mass loading of  $\text{Ni}_2(\text{OH})_2\text{CO}_3$  nanowires was washed by water and ethanol. The loading mass of  $\text{Ni}_2(\text{OH})_2\text{CO}_3$  on composite paper was 73wt% (comparing with the whole mass of the composite paper). The areal density of the composite paper was 14.60  $\text{mg cm}^{-2}$ , as a result, the areal loading amount of  $\text{Ni}_2(\text{OH})_2\text{CO}_3$  nanowires on CNT paper was 10.62  $\text{mg cm}^{-2}$ . The thickness of the composite paper was 0.356 mm, and the square resistance of it was 10.32  $\Omega \square^{-1}$ . As a result, the calculated in-plan conductivity of the composite paper was 272  $\text{S m}^{-1}$ . The hybrid paper (mass >6 mg) was then embedded into a piece of nickel foam and applied electrochemical cycles in a three-electrode system. After several cycles of cyclic voltammetry or charge/discharge, the electrochemical capacitive performance of the hybrid paper could be largely improved by the electrochemical conversion.

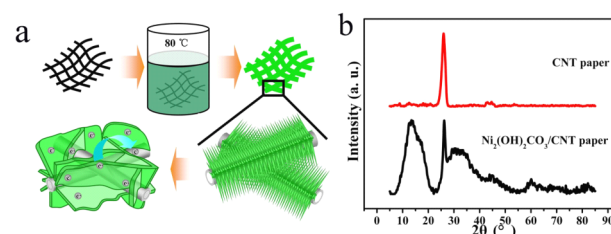


**Figure 1** the sketch map of the preparation process and the morphology change (a); XRD patterns of CNT paper before and after  $\text{Ni}_2(\text{OH})_2\text{CO}_3$  deposition (b).

Figure 1b shows the XRD patterns of CNT paper before and after  $\text{Ni}_2(\text{OH})_2\text{CO}_3$  deposition. This comparison reveals that the pristine CNTs have high crystallization. As reported in our previous researches, these MWCNTs prepared by floating catalyst chemical vapor deposition method have excellent graphite-like structures with tens of walls. This nanostructure was beneficial for the uniform growth of inorganic nanomaterials on these CNTs. After chemical growth process, the Ni based basic carbonate grown on CNT paper shows amorphous-like pattern as shown in Figure 1(b), which means that it may have ultra-thin crystal size. Comparing with PDF data base, the basic carbonate may

content  $\text{Ni}_2(\text{OH})_2\text{CO}_3$  and  $\text{Ni}_2(\text{OH})_2\text{CO}_3 \cdot \text{H}_2\text{O}$  (PDF#35-0501 and PDF#29-0868).

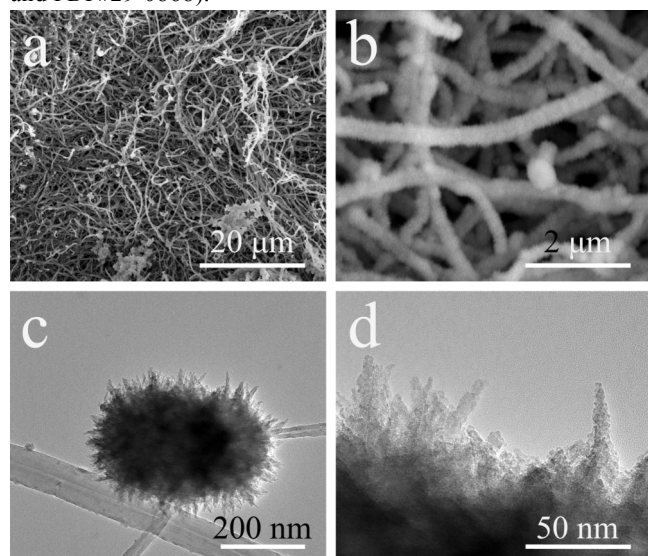


**Figure 2** SEM images (a,b) and TEM images (c,d) of  $\text{Ni}_2(\text{OH})_2\text{CO}_3$  nanowires on CNT paper.

The morphologies of  $\text{Ni}_2(\text{OH})_2\text{CO}_3$  nanostructures on CNT paper were shown in Figure 2(a) and 2(b). The results revealed that  $\text{Ni}_2(\text{OH})_2\text{CO}_3$  nanostructure existed as a nanowire arrays on the CNT paper. These nanowires are uniformly coated on individual CNTs to form a hierarchical core/shell structural nanowire structure, and do not change the open-porous nanostructure of the pristine paper. TEM images in Figure 2(c) and 2(d) shows that these nanowires have the diameter of fewer than 10 nm, and are formed by ultra-thin nanocrystals as a multi-crystal structure. From Figure S1 in supporting information, its crystal structure could not be clearly distinguished from high-resolution TEM image. This phenomenon was matched with its XRD pattern in Figure 1(b), which indicated that the  $\text{Ni}_2(\text{OH})_2\text{CO}_3$  has an amorphous structure. Other substrates such as small diameter MWCNTs, reduced graphene oxide (rGO) nanosheets, nickel foam and carbon fiber paper was chosen as the substrates to grow  $\text{Ni}_2(\text{OH})_2\text{CO}_3$  with the same method. The results are shown in Figure S2. Small-diameter MWCNTs could not serve as a suitable substrate to achieve mass growth of  $\text{Ni}_2(\text{OH})_2\text{CO}_3$  nanowire arrays. Only discontinuous nanowire coating was grown on individual CNTs as shown in Figure S2(a) and S2(b). It should be attributed to the small radius of curvature, which was not beneficial for the dense growth of nanowire arrays with the diameters not small enough. rGO nanosheets with flat structure were beneficial for the growth of nanowire arrays. However, as shown in Figure S2(c) and S2(d), the height of these nanowires are ultra-short, which should be attributed to the weak mechanical performance of individual rGO nanosheets and the dense aggregation of rGO, which may reduce the size of space for the hierarchical growth of nanowire arrays. As a result, the loading mass of  $\text{Ni}_2(\text{OH})_2\text{CO}_3$  nanowires on rGO may be limited. Macro sized nickel foam and carbon fiber paper have the surface with ultra-large radius of curvature, which was useful for the

growth of dense  $\text{Ni}_2(\text{OH})_2\text{CO}_3$  nanowire arrays. However, these arrays were too dense for electrolyte diffusion. The cracks in Figure S2(e) and S2(g) proved that these arrays could be easily separated with the substrates. Thus comparing with these substrates, large-diameter MWCNTs are must suitable substrates for the uniform growth of  $\text{Ni}_2(\text{OH})_2\text{CO}_3$  nanowire arrays for the suitable diameter of these CNTs.

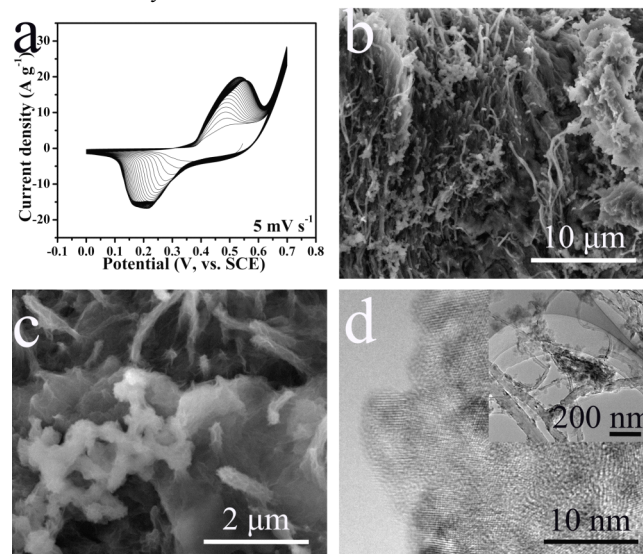


**Figure 3** CV cyclic curves of  $\text{Ni}_2(\text{OH})_2\text{CO}_3/\text{MWCNT}$  hybrid paper electrodes at  $5 \text{ mV s}^{-1}$  (a); SEM images of the hybrid paper after electrochemical cycles (b,c) and TEM images of the electrochemically converted  $\text{Ni}(\text{OH})_2$  nanosheets (d) (inserted image: CNTs with  $\text{Ni}(\text{OH})_2$  nanosheets).

The electrochemical performance of the  $\text{Ni}_2(\text{OH})_2\text{CO}_3/\text{MWCNT}$  hybrid paper electrode was investigated in 6 M KOH solution. Figure 3(a) shows CV curves of the sample with 50 cycles at a scan rate of  $5 \text{ mV s}^{-1}$ . The result indicated that the specific capacitance may be fast increased in initial several cycles. When the cycle number was near to 50, the capacitance increase became slow. After 50 cycles, the cycle area of the CV curves increased to more than 3 times comparing with the initial cycle. This phenomenon suggests that there may exist a phase conversion in  $\text{Ni}_2(\text{OH})_2\text{CO}_3$  nanostructures. Figure 3(b) shows the  $\text{Ni}_2(\text{OH})_2\text{CO}_3$  nanowire arrays had already be converted into nanosheets on individual CNTs, and these nanosheets joined together to form a hierarchical nanowire structure. They are thinner than  $\text{Ni}(\text{OH})_2$  nanosheets reported before. These thin nanosheets could effectively increase the contact area of the hydroxide with electrolyte, thus improve the specific area. TEM image in Figure 3(d) indicated that these nanosheets have excellent crystallization, which was largely different from the amorphous  $\text{Ni}_2(\text{OH})_2\text{CO}_3$  nanowires before electrochemical cycles. In another words, the electrochemical cyclic process converted  $\text{Ni}_2(\text{OH})_2\text{CO}_3$  to another phase. Comparing with PDF card data base, it could be conclude that most of the crystal faces belong to (001) face of  $\text{Ni}(\text{OH})_2$  (PDF#14-0117). From the inserted image of Figure 3(d), it could be estimated that the size of converted  $\text{Ni}(\text{OH})_2$  particle may be around 20 nm. As reported by Zhu et al, Ni/Co basic carbonate could be

converted to hydroxide nanosheets by immersing into 6 M NaOH aqueous solution for more than 18 h.<sup>10</sup> This process spent long time and the converted part was only on the surface of the nanowires but not include the inner parts. They indicated that this conversion was mainly an exchange between  $\text{CO}_3^{2-}$  in  $\text{Ni}_x\text{Co}_{2-x}(\text{OH})_2\text{CO}_3$  and  $\text{OH}^-$  in NaOH aqueous solution ( $0 \leq x \leq 2$ ). However, here we give out a new proper mechanism for the conversion of Ni/Co basic carbonate to Ni/Co hydroxide in an electrochemical cyclic process. There existed weak pseudocapacitive peaks in the initial cycle of CV curves in Figure 3(a). However, the intensity of the two peaks largely increased along with the cycles.  $\text{Ni}_2(\text{OH})_2\text{CO}_3$  crystal has its pseudocapacitive core  $\text{Ni}^{2+}$ , which could be converted to  $\text{Ni}^{3+}$  in electrochemical charge process, and the latter ion existed as  $\text{NiOOH}$ , which was converted by  $\text{Ni}_2(\text{OH})_2\text{CO}_3$ .  $\text{CO}_3^{2-}$  was resolved into the electrolyte and  $\text{NiOOH}$  kept as a solid on individual MWCNTs. In this process, amorphous  $\text{Ni}_2(\text{OH})_2\text{CO}_3$  nanowires were crystallized into  $\text{NiOOH}$  crystals, the latter existed as layered structure. After that, in the discharge process,  $\text{NiOOH}$  converted to  $\beta\text{-Ni}(\text{OH})_2$  and  $\text{CO}_3^{2-}$  was not existed in the solid phase on MWCNTs. As a result, the  $\text{Ni}(\text{OH})_2$  nanosheets were shown on individual CNTs as in Figure 3(b) and 3(c). The conversion equations are shown below.



Supposing that the conversion process happened completely, the mass of the composite paper could be decreased 9wt% for the exchange of  $\text{CO}_3^{2-}$  with two  $\text{OH}^-$  ions. As a result, the calculated content of  $\text{Ni}(\text{OH})_2$  in the composite paper was 70wt% comparing with 73wt% of  $\text{Ni}_2(\text{OH})_2\text{CO}_3$  in pristine composite paper as mentioned above. However, considering the aim of exhibiting the conversion process, the mass of the pristine composite paper was used to calculate the electrochemical performance.

This electrochemical conversion process spent fewer time than simply immersing, and could achieve total phase change from  $\text{Ni}_2(\text{OH})_2\text{CO}_3$  to  $\text{Ni}(\text{OH})_2$  with the help of electrons. Furthermore, they had MWCNTs as the conductive core, thus their electrochemical performance could be effectively improved. The CV curve comparison of Ni foam (after 100 cycles of CV at 5 mV s<sup>-1</sup>), converted  $\text{Ni}(\text{OH})_2/\text{rGO}$  and converted  $\text{Ni}(\text{OH})_2/\text{MWCNT}$  hybrid paper at the scan rate of 5 mV s<sup>-1</sup>. The results show that the two samples containing converted  $\text{Ni}(\text{OH})_2$  have a typical pair of pseudocapacitive peaks as  $\text{Ni}(\text{OH})_2$ , which was different from pristine Ni foam. Furthermore, the sample with MWCNT paper shows much larger cyclic area comparing with converted  $\text{Ni}(\text{OH})_2/\text{rGO}$  composite. It should be attributed to the low loading mass of pristine  $\text{Ni}_2(\text{OH})_2\text{CO}_3$  nanowires grown on rGO nanosheets.

CV curves of this sample at different scan rates are shown in Figure S3(a). The rate performance plots of the two samples are shown in Figure 4(b). The specific capacitance data of the samples were calculated from charge/discharge

curves (see Figure S3(b)) based on the mass of pristine composite paper. This comparison was agreed with CV curves in Figure 4(a). The specific capacitance of converted  $\text{Ni}(\text{OH})_2/\text{MWCNT}$  hybrid paper was 1517 F g<sup>-1</sup> at the current density of 0.5 A g<sup>-1</sup>, and kept 913 F g<sup>-1</sup> at 10 A g<sup>-1</sup>. The charge/discharge curves are shown in Figure S3(b), in which these curves show typical platforms for  $\text{Ni}^{2+}/\text{Ni}^{3+}$  conversion. As Zhu et al reported, the surface-converted  $\text{Ni}_{0.5}\text{Co}_{1.5}(\text{OH})_2\text{CO}_3@/\text{Ni}_{0.25}\text{Co}_{0.75}(\text{OH})_2$  core/shell structural nanowire array had a specific capacitance of 928.4 F g<sup>-1</sup> at 5 mA cm<sup>-2</sup>,<sup>10</sup> lower than the totally converted  $\text{Ni}(\text{OH})_2$  nanosheet/MWCNT hybrid paper, which reveals the advantage of electrochemical conversion strategy and the conductive MWCNT scaffold. Zhu et al reveals that the hierarchical  $\text{Ni}_2(\text{CO}_3)(\text{OH})_2 \cdot x\text{H}_2\text{O}$  nanospheres had a specific capacitance of 1178.2 F g<sup>-1</sup> at 0.5 A g<sup>-1</sup> and decreased to 612.8 F g<sup>-1</sup> at 10 A g<sup>-1</sup>,<sup>11</sup> which indicated that the simple mixing of Ni compounds powder with conductive filler and polymer binder could not have close interface between them, which largely limited the electrochemical performance of the electrodes. Comparing with the CNT@converted  $\text{Ni}(\text{OH})_2$  composite network, the similar structure based on CNT film/NiO nanonet/stainless steel has larger specific capacitance (1636 F g<sup>-1</sup> at 1 A g<sup>-1</sup>), higher rate performance but lower mass loading on the scaffold (0.37 mg).<sup>12</sup> Although directly growth of  $\text{Ni}(\text{OH})_2$  on CNT film could be simply achieved by chemical bath deposition as reported by Wang et al<sup>7</sup> and Hakamada et al<sup>13</sup> the thick  $\text{Ni}(\text{OH})_2$  nanosheets and nanoparticles with high crystallization and low defect density could limit the electrochemical performance of the electrodes. It indicated that the converted  $\text{Ni}(\text{OH})_2$  with finer nanostructures on CNT paper could effectively enhance the electrochemical performance of  $\text{Ni}(\text{OH})_2$ . Comparing with the growth of  $\text{Ni}(\text{OH})_2$  on CNT paper, the  $\text{Ni}(\text{OH})_2$  grown on CNT/Ni foam could largely enhance its electrochemical performance, but its loading mass on CNT/Ni foam was limited by the surface area of Ni foam.<sup>14</sup> Reduced graphene oxide (rGO) was also usually used to enhance the electrochemical performance of  $\text{Ni}(\text{OH})_2$  as the electrode of supercapacitors.<sup>15-18</sup> Their specific capacitance could be even more than 2000 F g<sup>-1</sup>.<sup>15</sup> However, these composites usually could not form paper electrodes.<sup>15-17</sup> The film state with graphene/ $\text{Ni}(\text{OH})_2$  had high areal capacitance, but the loading mass of  $\text{Ni}(\text{OH})_2$  could be limited by the sandwich structure.<sup>18</sup> The cyclic performance of the hybrid paper was shown in Figure 4(c), which also reveals the electrochemical conversion process in the first tens of cycles. The specific capacitance of the sample still kept higher than 1000 F g<sup>-1</sup> after 1000 cycles at 2 A g<sup>-1</sup>. The Nyquist plots of the sample before and after cyclic test were shown in Figure 4(d). This comparison indicated the large decrease of charge transfer resistance ( $R_{ct}$ ) and the clear Warburg impedance (electrolyte diffusion resistance) after 1000 cycles of charge/discharge. Both of the two phenomena reveal the conversion of amorphous  $\text{Ni}_2(\text{OH})_2\text{CO}_3$  nanowires to  $\text{Ni}(\text{OH})_2$  crystal nanosheets. The latter has higher conductivity and effective open-pore structures for electrolyte diffusion, which are the keys for the decrease of  $R_{ct}$  and Warburg impedance.

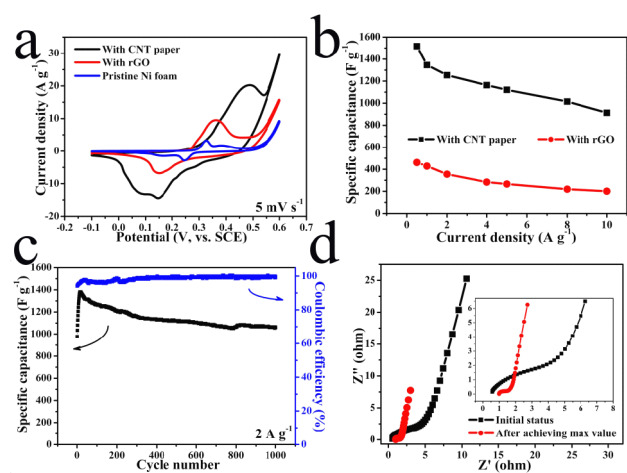


**Figure 4** CV curve comparison of Ni foam, converted Ni(OH)<sub>2</sub> with graphene and with MWCNT paper (a); Ni<sub>2</sub>(OH)<sub>2</sub>CO<sub>3</sub>/MWCNT hybrid paper electrodes at the scan rate of 5 mV s<sup>-1</sup> (a); rate performance of converted Ni(OH)<sub>2</sub> with graphene and with MWCNT paper (b); charge/discharge cyclic performance of converted Ni(OH)<sub>2</sub>/MWCNT hybrid paper at the current density of 2 A g<sup>-1</sup> (c); Nyquist plots of Ni<sub>2</sub>(OH)<sub>2</sub>CO<sub>3</sub>/MWCNT hybrid paper and converted Ni(OH)<sub>2</sub>/MWCNT hybrid paper (d).

In conclusion, the electrochemical converted Ni(OH)<sub>2</sub> nanosheets on MWCNT paper show superior performance as a binder-free pseudocapacitive electrode. This conversion process spent fewer times than immersing method, and achieved total phase change. Thus it could be beneficial for the design of high performance electrodes of supercapacitors.

This work was supported by the National Science Foundation of China (No.21203238), the National Basic Research Program (No. 2011CB932600-G), and Knowledge Innovation Program (KJCX2.YW.M12) of the Chinese Academy of Sciences.

## Notes and references

<sup>a</sup> Suzhou Institute of Nano-tech & Nano-bionics, Chinese Academy of Sciences, No.398 Ruoshui Road, Suzhou, P. R. China. Fax: 86 512 62872806; Tel: 86 512 62872806; E-mail: [mhchen2008@sinano.ac.cn](mailto:mhchen2008@sinano.ac.cn) and [qwli2007@sinano.ac.cn](mailto:qwli2007@sinano.ac.cn).

<sup>b</sup> Key Lab of Nanodevices and Applications, Suzhou Institute of Nano-Tech and Nano-Bionics, Chinese Academy of Sciences, Suzhou 215123, P. R. China.

<sup>c</sup> School of Materials Science and Engineering, Zhengzhou University, Zhengzhou, 450001, P. R. China.

<sup>d</sup> Nano Science and Technology Institute, University of Science and Technology of China, Suzhou, 215123, P. R. China.

<sup>e</sup> University of Chinese Academy of Sciences, Beijing, 100049, P. R. China.

† Electronic Supplementary Information (ESI) available: [Experimental details; HRTEM image of Ni<sub>2</sub>(OH)<sub>2</sub>CO<sub>3</sub> nanowires; SEM images of Ni<sub>2</sub>(OH)<sub>2</sub>CO<sub>3</sub> nanowire arrays grown on small-diameter MWCNTs, rGO nanosheets, carbon fiber paper and nickel foam; CV curves at different scan rates and charge/discharge curves at different current densities of converted Ni(OH)<sub>2</sub>/MWCNT hybrid paper]. See DOI: 10.1039/b000000x/

1 G. Yu, X. Xie, L. Pan, Z. Bao, Y. Cui, *Nano Energy*, 2013, **2**, 213; P. Simon, Y. Gogotsi, *Nat. Mater.*, 2008, **7**, 846.

- 2 A. Ghosh, Y. H. Lee, *Chem. Sus. Chem.*, 2012, **5**, 480; X. Li, B. Wei, *Nano Energy*, 2013, **2**, 159.
- 3 J. G. Chen, J. Q. Xiao., *Angew. Chem. Int. Ed.*, 2013, **52**, 1882.
- 4 Z. Tang, C. Tang, H. Gong, *Adv. Funct. Mater.*, 2012, **22**, 1272; J. Liu, Y. Ren, B. Dasgupta, H. Tanoto, H. L. Seng, W. K. Chim, S. F. Y. Li, S. Y. Chiam, *J. Mater. Chem. A*, 2013, **1**, 15095; S. Kim, P. Thiyagarajan, J. Jang, *Nanoscale*, 2014, accepted, DOI: 10.1039/c4nr02204a; I. C. Chang, T. T. Chen, M. H. Yang, H. T. Chiu, C. Y. Lee, *J. Mater. Chem. A*, 2014, **2**, 10370.
- 5 G. Hu, C. Li, H. Gong, *J. Power Sources*, 2010, **195**, 6977.
- 6 N. A. Alhebshi, R. B. Rakhi, H. N. Alshareef, *J. Mater. Chem. A*, 2013, **1**, 14897.
- 7 L. Wang, H. Chen, F. Cai, M. Chen, *Mater. Lett.*, 2014, **115**, 168.
- 8 H. Wang, H. S. Casalongue, Y. Liang, H. Dai, *J. Am. Chem. Soc.*, 2010, **132**, 7472.
- 9 Y. Jin, H. Chen, M. Chen, N. Liu, Q. Li, *ACS Appl. Mater. Interfaces*, 2013, **5**, 3408.
- 10 W. Zhu, Z. Lu, G. Zhang, X. Lei, Z. Chang, J. Liu, X. Sun, *J. Mater. Chem. A*, 2013, **1**, 8327.
- 11 G. Zhu, C. Xi, M. Shen, C. Bao, J. Zhu, *ACS Appl. Mater. Interfaces*, 2014, **6**, 17208.
- 12 M. Wu, Y. Zheng, G. Lin, *Chem. Commun.*, 2014, **50**, 8246.
- 13 M. Hakamada, A. Moriguchi, M. Mabuchi, *J. Power Source.*, 2014, **245**, 324.
- 14 Z. Tang, C. Tang, H. Gong, *Adv. Funct. Mater.*, 2012, **22**, 1272.
- 15 J. Yan, W. Sun, T. Wei, Q. Zhang, Z. Fan, F. Wei, *J. Mater. Chem.*, 2012, **22**, 11494.
- 16 J. Yan, Z. Fan, W. Sun, G. Ning, T. Wei, Q. Zhang, R. Zhang, L. Zhi, F. Wei, *Adv. Funct. Mater.*, 2012, **22**, 2632.
- 17 Y. Wang, S. Gai, N. Niu, F. He, P. Yang, *J. Mater. Chem. A*, 2013, **1**, 9083.
- 18 J. Xie, X. Sun, N. Zhang, K. Xu, M. Zhou, Y. Xie, *Nano Energy*, 2013, **2**, 65.